

# Estimation of Elastic Deformations and Fracture Peripheral Speeds of Grinding Wheels due to Centrifugal Forces by Means of Grinding Wheels Model

Takazo Yamada<sup>1</sup>, Hwa-Soo Lee<sup>1</sup>

<sup>1</sup>Dept. of Mechanical Engineering, Nihon University, Japan

E-mail: yamada@mech.cst.nihon-u.ac.jp

[Received May 1, 2012; Accepted September 30, 2012]

## Abstract

In grinding operation, centrifugal forces act to grinding wheels, and expand and/or deform the grinding wheels. Additionally, in high rotating speeds, grinding wheels are destroyed by the centrifugal force in case of that centrifugal force is over fracture strength of grinding wheel. In this study, in order to obtain elastic deformations and fracture peripheral speeds of grinding wheel, grinding wheel model is proposed. And, it is clarified that elastic deformations of grinding wheel and fracture peripheral speeds of grinding wheel can be calculated using grinding wheel model and FEM analysis without actual rotating tests.

Keywords: Grinding wheels model, Centrifugal force, Elastic deformation, Fracture peripheral speed, Three points bending test

## 1 INTRODUCTION

Grinding wheels are influenced by centrifugal forces in grinding operation. Since grinding wheels are expanded by this centrifugal force, elastic deformations of grinding wheels effect on the form tolerance of ground workpiece. Additionally, in high rotating speeds, grinding wheels are broken by the effect of the centrifugal forces. In order to keep the safety in machining shops, rotating speeds of wheels have to be considered sufficiently. However, in definition of maximum rotating speed, wheel makers are performing actual fracture tests to evaluate the fracture speeds for their products. Although, fracture test results using actual wheels are reliable, performing fracture tests take a lot of cost and time.

Study on the elastic deformations of grinding wheels due to centrifugal forces have been done by Saito using the stress distribution acting grinding wheel [1]. On the other hand, studies on the fracture of grinding wheels have been carried out by Shionozaki, Yamamoto, Inoue and Suzuki, in which theories of maximum stress, mean stress and/or the minimum probability are applied under the condition that wheels are assumed to be rotating uniform continuous plates [2]-[5]. Although, elastic deformations and/or fracture condition of grinding wheels due to centrifugal forces are clarifying from above studies, one of the problem in these studies is that grinding wheels are regarded as uniform continuous body. Since, as well known, grinding wheels consist of abrasive grains and bond-bridges, it is considered that actual elastic deformations and/or fracture condition of grinding wheels cannot be obtained by assumption that grinding wheels are regarded as uniform continuous body.

On the other hand, in our studies, a mathematical model of grinding wheels was proposed in order to analyze various kind of elastic phenomena of grinding wheels under machining, so far [6][7]. In this model, it is assumed that grains are rigid bodies and bond-bridges are spring elements. Spring constant of spring element can be obtained by three points bending tests using abrasive

sticks. Applying various load of grinding operation to proposed model, elastic deformations of grinding wheels during grinding can be calculated by analysis.

From such a viewpoint, this study aims to estimate the elastic deformation and the fracture peripheral speed of grinding wheel by applying centrifugal forces to this proposed model. Using measured results of spring constant of spring element as bond-bridge for vitrified and resinoid wheels with grain size from 60 to 120, targeted grinding wheel are modeled. Comparing analyzed results with measured results of elastic deformation and fracture speed, the validity of estimation method of these phenomena of grinding wheel is shown. From estimation of fracture peripheral speed in particular, it is confirmed that dangerous fracture tests using actual grinding wheels don't need in wheel makers.

## 2 GRINDING WHEELS MODEL AND STATIC STIFFNESS OF BOND-BRIDGE

### 2.1 GRINDING WHEELS MODEL

Grinding wheels consist of abrasive grains, bonds and pores as shown in figure 1(a). In this study, a mathematical model of grinding wheels as shown in figure 1(b) was proposed [6][7]. In this model, it is assumed that grains are rigid bodies and bond-bridges are spring elements. Spring constant of spring element can be regarded as a static stiffness of bond-bridge. A basic unit consists of nine rigid bodies and sixteen spring elements as shown in figure 1(b). Diameter of abrasive grain  $D$  and distance between successive two grains  $A$  in this model can be shown as follows by using grain size  $G$  and volume percentage of grain  $V$ .

$$D = 45G^{-1.28} \quad (1)$$

$$A = \sqrt[3]{\frac{\pi}{3\sqrt{2}V}} D \quad (2)$$

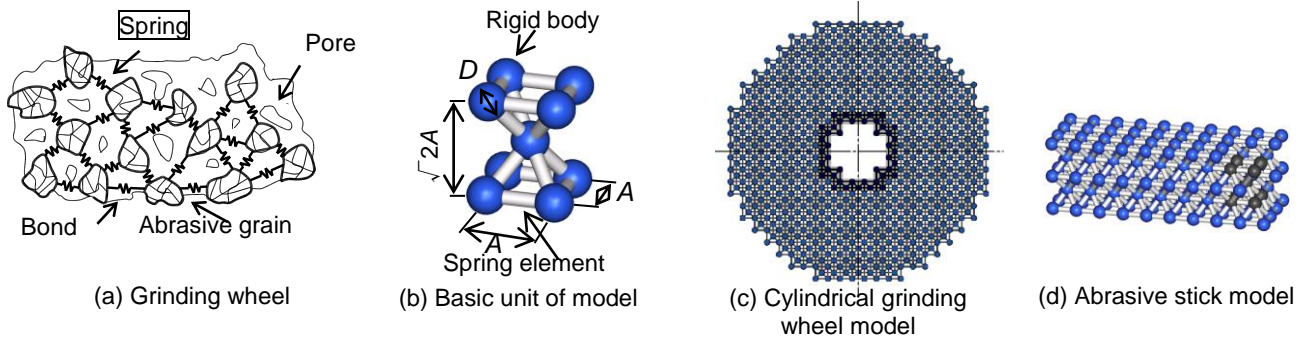


Figure 1: Proposed grinding wheel model

Arranging this basic unit, cylindrical grinding wheels and abrasive sticks as shown in figure 1(c) and (d) can be easily modeled.

## 2.2 MEASUREMENT OF STATIC STIFFNESS OF BOND-BRIDGE BY MEANS OF THREE POINTS BENDING TEST

Spring constant regarded as the static stiffness of bond-bridge  $k$  can be obtained by finite element method and three points bending test as follows.

In three points bending test by means of abrasive stick model as shown in figure 1(d), abrasive stick model loaded by bending load  $F$  occurs elastic deformation  $\delta$ . Although abrasive stick model consists of a lot of spring element, the relation among load  $F$ , deformation  $\delta$  and stiffness  $k$  taking into account only one loading direction can be shown as follow.

$$F = \alpha k \delta \quad (3)$$

Where,  $\alpha$  is called a geometrical coefficient of grinding wheel in this study.  $\alpha$  is changed by the number of spring element and/or arrangement of element. However,  $\alpha$  is constant in case of the same shape model, and isn't depended on the spring constant of spring element. Therefore, if the relation between load  $F$  and deformation  $\delta$  can be obtained by analysis using three points bending test under the certain spring constant  $k$ ,  $\alpha$  can be calculated by substituting  $F$ ,  $\delta$  and  $k$  in equation (3).

The static stiffness  $k$  is calculated as follows. In the method shown above,  $\alpha$  was calculated under the certain spring constant  $k$ . Actual stiffness  $k$  can be obtained by three points bending test using actual abrasive stick. From three points bending test, actual relation between load  $F$  and deformation  $\delta$  can be measured. Therefore, substituting  $F$ ,  $\delta$  and  $\alpha$  in equation (3), actual spring constant, that is the static stiffness of bond-bridge  $k$ , can be obtained quantitatively.

Bending tests using vitrified and resinoid wheels for grain size #60, #80, #100 and #120, hardness grade J, structure 6 are carried out. The sizes of used abrasive sticks are shown in table 1.

In finite element method, both ends of abrasive stick model are held by simple support, and center of model is loaded by concentrated load  $F$ . On the other hand, abrasive stick can be modeled by grinding wheel's indication. For example, in case of grain size #60 and structure 6, diameter of abrasive grain  $D$  can be calculated from equation (1) as 0.238 mm. Since structure 6 is volume percentage of grain  $V=50\%$ , distance between successive two grains  $A$  can be calculated from

Table 1: Size of abrasive stick

Stick No.	Width mm	Height mm	Length mm
1	8.0	5.7	40
2	4.0	5.7	40
3	5.0	7.1	40

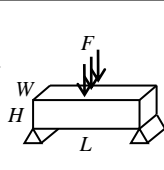
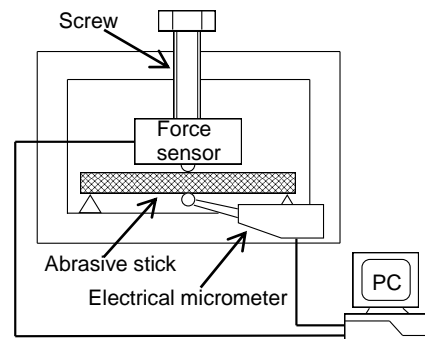



Figure 2: Schematic diagram of three points bending test

equation (2) as 0.271 mm.

Figure 2 shows a schematic diagram of three points bending test. The concentrated load is loaded by a screw and is measured by a force sensor. Elastic deformation is measured with an electric micrometer in the opposite side of the loading face. Since it is difficult to identify the initial contact point of loading bar to abrasive stick, relative load and displacement are monitored.

Figure 3 shows results of the three points bending test, in which vitrified wheels #60 and 50% are used. Substituting measured results  $F/\delta$  as shown in figure 3 and calculated results  $\alpha$  into equation (3), the static stiffness of bond-bridge  $k$  is calculated.

Figure 4 shows the relations between the static stiffness  $k$  and the grain size for vitrified and resinoid bonds. From this figure, it is known that the static stiffness  $k$  decreases with the increase of the grain size. This tendency may be caused by size effect of bond-bridge. That is, since bond-bridge shape decreases with the decrease of the abrasive grain diameter, the static stiffness  $k$  decreases with the increase of the grain size and/or the decrease of the abrasive grain diameter.

From these results of analysis and experiment, grinding wheel can be modeled using static stiffness  $k$ . So, in next stage, analyses of elastic deformation of grinding wheel and fracture peripheral speed due to centrifugal force are carried out using proposed model.

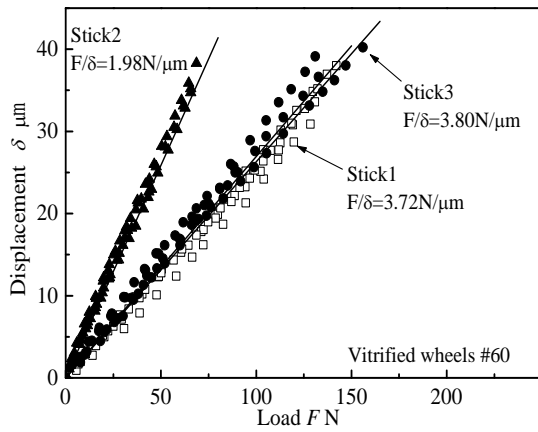


Figure 3: Results of three points bending tests

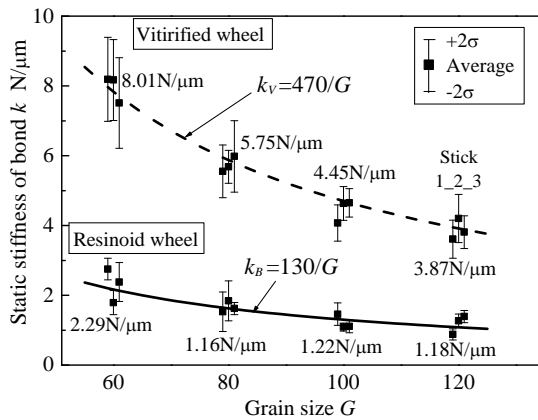


Figure 4: Relationship between grain size and static stiffness of bond-bridge

### 3 ESTIMATION OF ELASTIC DEFORMATIONS OF GRINDING WHEELS DUE TO CENTRIFUGAL FORCES

#### 3.1 MODELING AND MEASURING METHOD

In proposed grinding wheels model, it was known that spring constant of spring model as the static stiffness of bond-bridge could be obtained from above method. On the other hand, since the mass of bond-bridge as spring element cannot be considered in this model, whole masses of wheel are assumed to be uniformly distributed to each grains consisting of wheel. Therefore, mass of one abrasive grain considered mass of bond can be obtained from dividing mass of abrasive stick by number of abrasive grain. Table 2 shows the calculated results of mass of each grain under above assumption.

Figure 5 shows the condition of this analysis. Taking into account the geometrical symmetry, analyzing model can be treated in quarter. In this model, the inside boundary is

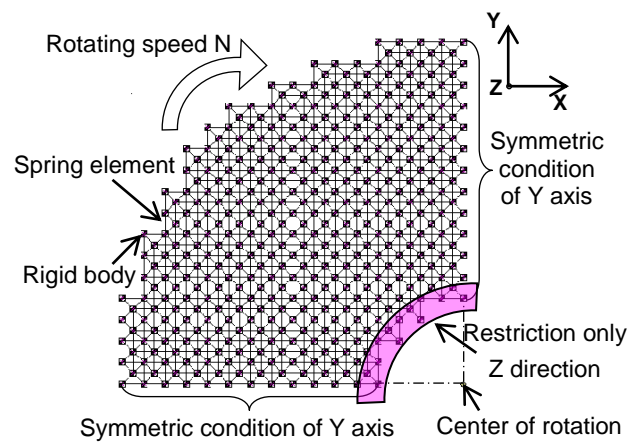


Figure 5: Condition of analysis

Table 3: Grinding wheel size and condition

Grain size	#60	#80	#100	#120
External dia.	100,150,205mm	100mm		
Internal dia.	50.8mm			
Rotating speed	2800min <sup>-1</sup>			
Peripheral speed	φ100: 880m/min, φ205: 1803m/min			

restricted in the Z axis directing the wheel spindle, and symmetric condition is set in X and Y directions. The elastic deformations in radial directions are calculated under the condition that spindle rotating speed is N min<sup>-1</sup>. Table 3 shows the condition used in this analysis.

On the other hand, the elastic deformation of the grinding wheels in radial direction is experimentally measured under the condition that diameter is 205 mm and rotating speed is 2800 min<sup>-1</sup>. Measuring method is as follows. Using acrylic resin plate for specimen, grinding wheel shapes in low and high rotating speeds are copied to the specimen surfaces. First, a flat surface is made on the specimen. Next, a groove is made under the condition that spindle rotating speed is 250min<sup>-1</sup> as shown section A-A in figure 6(a). Next, keeping the same depth of cut and increasing the spindle rotation speed to 2800min<sup>-1</sup>, a new groove is made on the previously ground groove as shown section B-B. The geometrical shapes of the section of two grooves are measured by a form measuring device as shown in figure 6(b) and (c). Finally comparing these measured two sections, the amounts of elastic deformations due to centrifugal force is evaluated.

#### 3.2 ANALYZED RESULTS AND MEASURED RESULTS

Figure 7 shows analyzed results and measured results of the elastic deformations due to centrifugal force for each grain size [8]. Here, in analyzed results, since proposed

Table 2: Mass of one abrasive grain considered mass of bond

Grain size	Resinoid wheels				Vitrified
	#60	#80	#100	#120	#120
Size of abrasive stick	8.0×5.7×60.2				
Mass of abrasive stick	6.01g	5.82g	5.82g	5.79g	5.92g
Number of abrasive grain	177051	483466	1389544	2258804	2258804
Mass of one abrasive grain considered mass of bond	0.0339mg	0.0120mg	0.00419mg	0.00256mg	0.00262mg

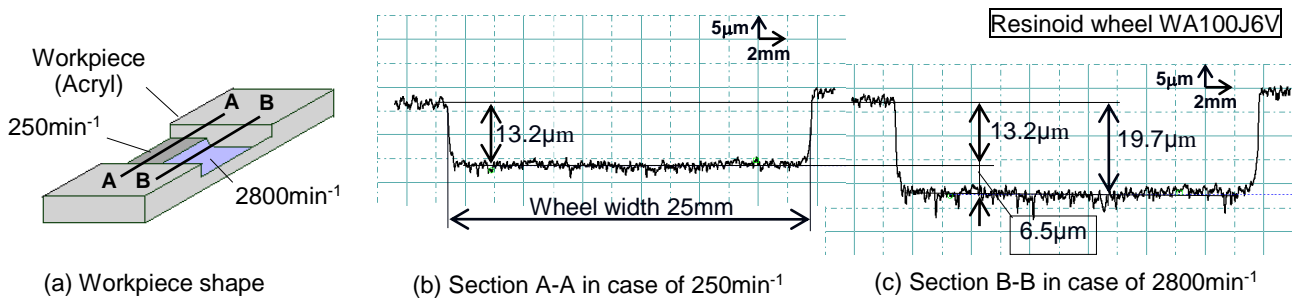


Figure 6: Workpiece shape and measured results of groove

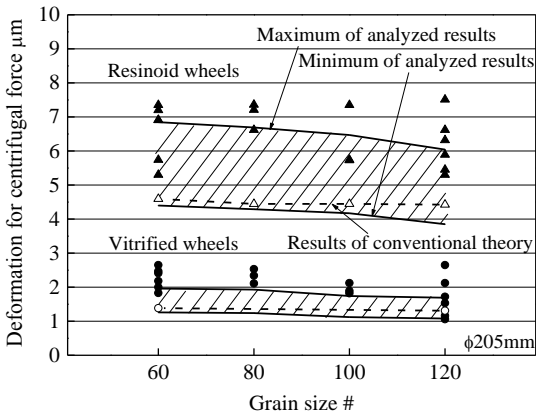


Figure 7: Results of deformations of grinding wheel

model has anisotropy itself, deformation is not uniform. And then, figure 7 shows the maximum and the minimum amounts of analyzed results. In this figure, plots show the experimental results and lines show the analyzed result. From experimental results for grain size 60, it may be known that elastic deformations are 1.5-2.5  $\mu\text{m}$  for vitrified wheels and 5.0-7.5  $\mu\text{m}$  for resinoid wheels. Comparing with analyzed results, it is known that experimental results are almost same amounts with the maximum amounts of analyzed results. These maximum amounts of analyzed results indicate the elastic deformation in lowest stiffness directions. Since, as well known, actual grinding wheel is not isotropic body, it can be considered that the elastic deformation due to centrifugal force may not be uniform in any directions. On the other hand, since the most external shapes of grinding wheel are copied to the surface of acrylic resin, experimental results shown in figure 7 are almost same amounts of the maximum analyzed results. Therefore, in order to obtain the elastic deformations of grinding wheel due to centrifugal force, it is known that maximum amounts have to be selected from analyzed results.

From these results, it is clarified that the elastic deformations due to centrifugal force can be calculated quantitatively using proposed model.

#### 4 ESTIMATION OF FRACTURE PERIPHERAL SPEEDS OF GRINDING WHEELS DUE TO CENTRIFUGAL FORCES

##### 4.1 DECISION OF FRACTURE CONDITION OF BOND

In higher rotating speed, grinding wheels are broken by higher centrifugal forces. So, in next stage, fracture condition, that is fracture peripheral speed has to be calculated from proposed model.

At first, fracture condition in proposed model has to be discussed. Rotating stress can be separated to a tangential stress and a radial stress. From conventional rotary disk theory, it is known that the tangential stress is higher than the radial stress, and maximum stress occurs in the disk inside area. On the other hand, analyzed result based on the proposed model shown in figure 5 also shows that maximum stress takes place in the inside area. From these results, becoming the stress in this model is greater than the fracture stress acting spring element in wheel, wheel fracture takes place. In such a consideration, the fracture force acting spring element is calculated as the first step of fracture analysis.

In this proposed model, a force acting spring element in rotating analysis is defined as an element force  $P$ . Similarly, the fracture force acting spring element when grinding wheel is fractured is defined as an element fracture force  $P_b$ . In case of that the element force  $P$  is larger than the element fracture force  $P_b$  in rotating analysis, it is regarded that grinding wheel is fractured by centrifugal force.

The element fracture force  $P_b$  can be calculated by finite element method using three points bending test of abrasive sticks. Fracture takes place at the center of bottom in abrasive stick in which the maximum stress occurs as shown in figure 8(a). Here, three points bending tests were carried out until abrasive sticks were broken as shown in figure 3. Therefore, fracture force of abrasive stick  $F_b$  can be obtained from figure 3. Table 4 shows

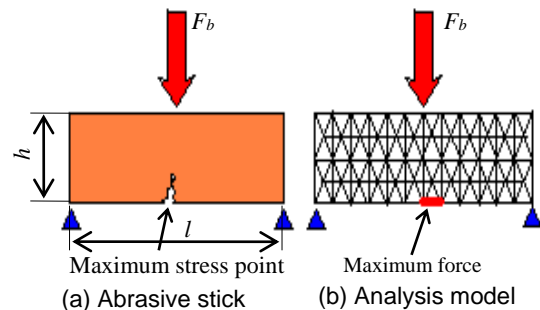


Figure 8: Three point bending test and analysis

Table 4: Results of three points tests

Stick No.	Fracture force $F_b$			
	#60	#80	#100	#120
1	144N	133N	220N	195N
2	70N	66N	100N	98N
3	155N	143N	207N	165N

measured results of fracture force  $F_b$  for each abrasive stick.

In analyses of three points bending test as show in figure 8(b), the center of abrasive stick models are loaded by obtained fracture forces  $F_b$  as shown in table 4. In this model, maximum force takes place at the spring element locating on the center of bottom in abrasive stick. Therefore, maximum force of this element can be obtained as the element fracture force  $P_b$  of grinding wheel model. Figure 9 shows the relation between grain size and the element fracture force  $P_b$ . From this figure, it is known that the element fracture force  $P_b$  decreases with the increase of grain size without any dispersion. It may be considered that since the volume of bond decreases with the increase of grain size, bonds become easier to be broken by smaller forces. Taking into account the tendency shown in figure 9, the average amount of each test piece is treated as the element fracture force  $P_b$  for each grain size.

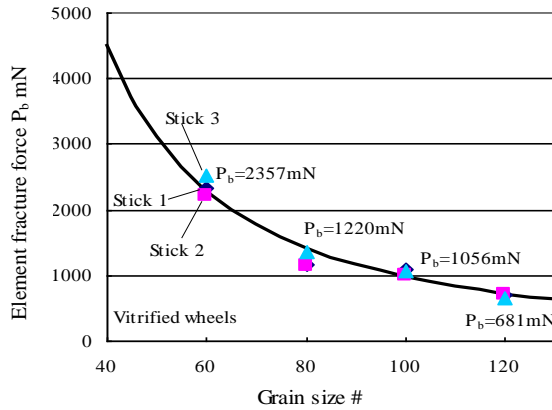


Figure 9: Relation between grain size and fracture force

#### 4.2 ANALYSIS METHOD OF FRACTURE PERIPHERAL SPEED

Relation between the element force  $P$  and the peripheral speed  $V$  can be obtained as follows. Tangential stress  $\sigma_\theta$  for the uniform continuous body under the rotating can be calculated by next equation from the rotating disk theory.

$$\sigma_\theta = \frac{3+\nu}{8} \rho \omega^2 \left\{ r_a^2 + r_b^2 - \frac{1+3\nu}{3+\nu} r^2 + \frac{r_a^2 r_b^2}{r^2} \right\} \quad (4)$$

Where  $\nu$  is Poisson' ratio,  $\rho$  is density,  $\omega$  is angular velocity,  $r_a$  is internal radius,  $r_b$  is external radius and  $r$  means a certain radius. In equation (4), assumed that the tangential stress  $\sigma_\theta$  is a stress acting each spring element in tangential direction as shown in figure 10, the tangential stress  $\sigma_\theta$  can be obtained from dividing the element force  $P$  by bond's cross section  $A$ . On the other hand, angular velocity  $\omega$  can be obtained from dividing peripheral speed  $V$  by external radius  $r_b$ . Substituting these relations in equation (4), relationship between the element force  $P$  and peripheral speed  $V$  can be obtained as follow.

$$P = \left[ A \frac{3+\nu}{8} \rho \frac{1}{r_b^2} \left\{ r_a^2 + r_b^2 - \frac{1+3\nu}{3+\nu} r^2 + \frac{r_a^2 r_b^2}{r^2} \right\} \right] V^2 \quad (5)$$

Since  $A$ ,  $\nu$ ,  $\rho$ ,  $r_a$ ,  $r_b$  and  $r$  are constant, equation (5) can be shown using constant  $C$  as follow.

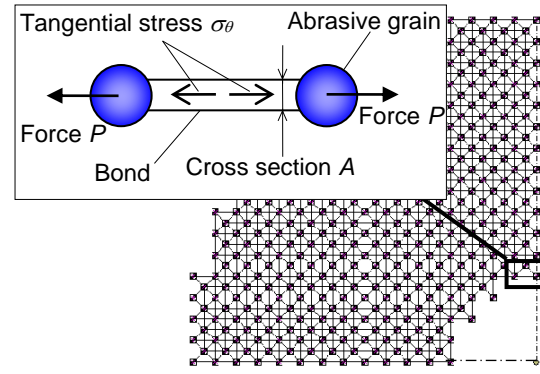


Figure 10: Tangential stress for bond-bridge

$$P = CV^2 \quad (6)$$

Similarly, the relation between the element fracture force  $P_b$  and fracture peripheral speed  $V_b$  can be shown as follow.

$$P_b = CV_b^2 \quad (7)$$

From equations (6) and (7), the relation among  $P$ ,  $P_b$ ,  $V$  and  $V_b$  is as follow.

$$V_b = \sqrt{\frac{P_b}{P}} V \quad (8)$$

As shown in above, the element fracture force  $P_b$  can be obtained from the three points bending test as shown in figure 9. The element force  $P$  under any peripheral speed  $V$  can be obtained using proposed model. Therefore, the fracture peripheral speed  $V_b$  can be calculated by substituting  $P_b$ ,  $P$  and  $V$  in equation (8).

#### 4.3 ANALYZED RESULTS AND DISCUSSION

Figure 11 shows relation between internal diameter and the element force  $P$  obtained by analyses for peripheral speed  $V$  as 6180 m/min. Here, the sizes of wheels are determined as follows. That is, the ratios of internal and external diameters  $i$ , = internal diameter / external diameter, are 0.376, 0.423, 0.476 and 0.544. Where, the range of internal diameter is from  $\phi 10$  to  $\phi 110$  mm.

Substituting  $P$  and  $V$  as shown in figure 11 and the element fracture force  $P_b$  as shown in figure 9 into equation (8), the peripheral fracture speed  $V_b$  can be

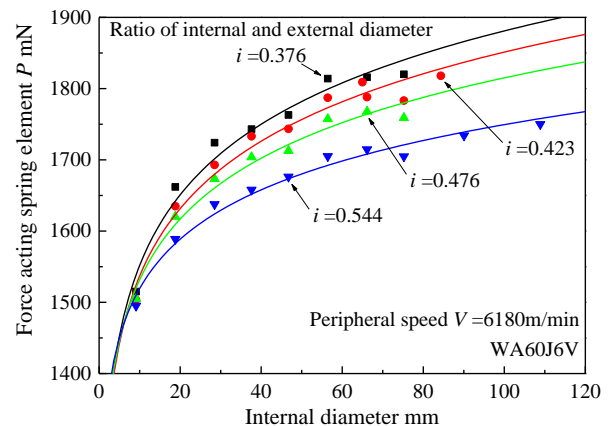


Figure 11: Relation between internal diameter and force acting spring element

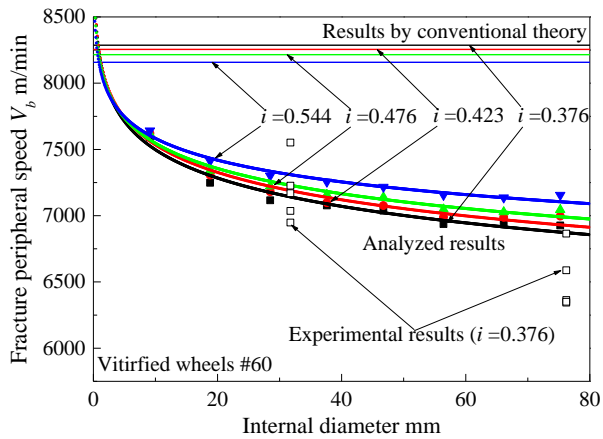


Figure 12: Relation between internal diameter and fracture peripheral speed

calculated. Figure 12 shows calculated results of peripheral fracture speed  $V_b$  for grain size 60. Here, in this figure, the fracture peripheral speeds  $V_t$  calculated by conventional theory as follow equation are also shown.

$$V_t = \sqrt{\frac{4\sigma_b}{\rho\{(1-\nu)i^2 + (3+\nu)\}}} \quad (9)$$

Where,  $\sigma_b$  is fracture stress of grinding wheel, and can be obtained by three points bending test of abrasive stick [9].

Comparing analyzed results and conventional theory as shown in figure 12, it is known that fracture peripheral speeds obtained by the analysis are lower than results of conventional theory. Since the conventional theory is intended for the uniform continuous body, stress of rotating disk acts uniformly. However, since grinding wheel consists of abrasive grains and bond-bridges, stress of grinding wheel concentrates to any bond-bridge and is larger than stress of rotating disk obtained by conventional theory. Therefore, since the centrifugal forces concentrate to one bond-bridge, it is considered that analysis results of fracture peripheral speed are smaller than calculated results used by conventional theory.

Figure 12 also shows experimental results used actual grinding wheels for  $i=0.376$  and internal diameters  $\phi 31.75$  and  $\phi 76.2$ . Experiment carried out using five grinding wheels for each size. From this figure, it is known that experimental results agree with analyzed results, and differ from calculated results using conventional theory. And, it is known that fracture peripheral speed decreases with the increase of internal diameter. This tendency also coincides with analyzed result. Since calculation of fracture peripheral speeds using the conventional theory differ from analyzed results and experimental results, it is considered that grinding wheel cannot be accepted as uniform continuous body, and fracture peripheral speed cannot be calculated by conventional theory. On the other hand, since this proposed model focuses on the fracture force of bond-bridge, it is considered that analyzed results agree with experimental results.

As shown above, it is clarified that using the proposed model, fracture speed of grinding wheel can be estimated quantitatively.

## 5 CONCLUSIONS

Using proposed model, elastic deformations of grinding wheels due to centrifugal forces were calculated. Since analyzed results coincide with experimental results, it is clarified that proposed model can apply to quantitative calculation of elastic deformation of grinding wheel. From analyzed results using vitrified wheel model and resinoid wheel model for grain size from 60 to 120, it is known that elastic deformations of vitrified wheel and resinoid wheel for diameter as  $\phi 205$  mm in rotating speed  $1800 \text{ min}^{-1}$  are  $1.5\text{-}2.5 \mu\text{m}$  and  $5.0\text{-}7.5 \mu\text{m}$ .

Estimation method of the fracture peripheral speeds of grinding wheels due to centrifugal forces was proposed using grinding wheel model. From this method, fracture peripheral speed can be obtained from analysis and only measured results of three points bending test using actual abrasive stick. From analyzed results agree with experimental results, it was shown that proposed method was appropriate. Using grinding wheel model, fracture peripheral speed can be obtained from analysis and three points bending test without dangerous fracture test using actual grinding wheel.

## REFERENCES

- [1] Saito, K., Kagiwada, T., 1978, Thermal deformation and thermal stress in the grinding wheel due to the grinding heat, The Japan Society of Mechanical Engineering, Vol.44, No.386, pp3622-3631.
- [2] Shonozaki, T., Matumoto, T., Shigematu, H., 1969, On the Bursting of Rotating Grinding Wheel, Journal of the Japan Society for Precision Engineering, 35, 11, 733.
- [3] Inoue, H., 1972, On Presumption of Strength of Centrifugal Rupture of Vitrified Grinding Wheel, Journal of the Japan Society for Precision Engineering, 37, 2, 105.
- [4] Suzuki, K., 1972, Development of Fracture Test Device of Grinding Wheel, Journal of the Japan Society for Precision Engineering, 38, 4, 405.
- [5] Yamamoto, A., Hori, M., Ueda, T., 1970, Rotating fracture Stiffness of grinding wheel, The Japan Society of Mechanical Engineering, 3, 36, 284, 655.
- [6] Yamada, T., Lee, H.S., Sadasue, K., Ito, Y., 2003, Study on Elasticity of Grinding Wheels (Modeling and Calculating the Stiffness of Grinding Wheels), The Japan Society of Mechanical Engineering, C, 69, 683, 1993.
- [7] Yamada, T., Lee, H.S., Shikauchi, T., Matsushita, H., 2002, Identification of the Static Stiffness of Grinding Wheels with Resin Bond, Proceeding of the ASPE 2002 Annual Meeting, 521.
- [8] Yamada, T., Lee, H.S., 2005, Study on elastic deformations of grinding wheels due to centrifugal forces by means of the grinding wheels model consisting of abrasive grains and bonds, Journal of the Japan Society for Abrasive Technology, 49, 10, pp.576-581.
- [9] Yamada, T., Lee, H.S., 2007, Estimation of the fracture peripheral speed of grinding wheels by means of grinding wheels model, Journal of the Japan Society for Abrasive Technology, 51, 10, pp.593-598.